Mechanics of Materials 43 (2011) 567–573

Contents lists available at ScienceDirect

Mechanics of Materials

journal homepage: www.elsevier.com/locate/mechmat

Nonuniform cleavage cracking across persistent grain boundary

W. Lu [a], J. Chen [a], X. Kong [b], S.S. Chakravarthula [b], Y. Qiao [a,*]

[a] Department of Structural Engineering, University of California – San Diego, La Jolla, CA 92093-0085, USA
[b] Department of Civil Engineering, University of Akron, Akron, OH 44325, USA

ARTICLE INFO

Article history:
Received 10 November 2010
Received in revised form 24 June 2011
Available online 21 July 2011

Keywords:
Grain boundary
Cleavage
Nonuniform
Fracture resistance

ABSTRACT

The nonuniform characteristics of cleavage cracking across high-angle grain boundaries are analyzed in considerable detail. To break through a grain boundary, a cleavage front would first penetrate across the boundary at its central part, with the side sections being locally arrested. Such a front behavior causes a strong crack trapping effect and a large increase in required crack growth driving force. Eventually, as the persistent grain boundary areas are separated apart, the crack front bypasses the grain boundary. The critical condition of the unstable crack propagation is determined by both the local fracture resistance and its increase rate with respect to the expansion of the break-through window. The grain boundary toughness is dominated by the effective grain boundary ductility.

1. Introduction

Accurately predicting fracture toughness of structural materials has been an active research area for many decades (McClintock and Argon, 1966). For intrinsically brittle materials, when the temperature is much higher than the brittle-to-ductile transition (BDT) temperature, significant plastic deformation can occur at crack tips. Therefore, the material tends to be ductile and the fracture work associated with crack propagation is quite large (Nemat-Nasser, 1981; Dodd and Bai, 1987). A typical ductile fracture process is related to microvoids formation and growth, leading to a fibrous appearance of fracture surfaces (Colangelo and Heiser, 1987). The fracture surface orientation is somewhat independent of the crystalline structure (Hull, 1999).

When the temperature is much lower than the BDT temperature, plastic deformation becomes difficult. Thus, the cracks often propagate in cleavage mode (Neimitz and Galkiewicz, 2010). The fracture toughness is much reduced and the material becomes brittle. Under this condition, the fracture surface consists of a number of smooth cleavage facets inside grains.

When the temperature is around the BDT temperature, the appearance transition and the fracture resistance transition do not always occur simultaneously (Chen et al., 1997). In many cases, while the fracture appearance is still dominated by cleavage facets, the fracture toughness is much higher than that at the lower shelf of the BDT region, close to or even higher than that of the fibrous fracture mode (Wu et al., 2003; Neimitz et al., 2010). Since usually few evidences of plastic deformation, such as plastic bending of cleavage ligaments, can be observed in cleavage facets inside a grain, the large fracture work must be associated with the grain boundary behaviors (Kang, 1999), especially when the cleavage crack propagation happens after extended plastic deformation.

In a theoretical analysis conducted by McClintock (1997), the contributions of grain boundary plastic shearing and mode-II fracture are discussed. As the two grains at both sides of a high-angle grain boundary are cleaved, further increase in crack opening load would cause the shear deformation in the grain boundary affected zone, accompanied by the nucleation and growth of boundary cracks. The length of the boundary crack can be assessed as $a_{cw} \cdot w$, where w is the crack opening displacement and a_{cw} is an analog to the punching operation factor, typically in the range of 0 to 3.6 (Lyman, 1969). The total

* Corresponding author.
E-mail address: yqiao@ucsd.edu (Y. Qiao).

0167-6636/$ - see front matter © 2011 Elsevier Ltd. All rights reserved.
doi:10.1016/j.mechmat.2011.07.001

fracture work caused by grain boundary plastic shear can be calculated as $k \cdot D_g h_0^2/[2(1+2a_{cw})]$, where k is the shear strength, D_g is the grain size, and $h_0 = 0.32D_g$ is the effective height of grain boundary ligament. The accumulative grain boundary fracture work leads to an effective fracture toughness, K_{gb1}, as high as 18 MPa $m^{1/2}$. This value is larger than the critical stress intensity factor associated with the crystallographic growth of cleavage crack, which is usually only 1–2 MPa $m^{1/2}$ (Wiesner, 1996). However, it is still much smaller than most of the experimental data of cleavage-like high-toughness fracture. For instance, at a relatively low temperature, while the majority of the fracture surfaces of a decarburized 1010 steel was cleavage facets, the fracture toughness was around 120 MPa $m^{1/2}$ (Qiao and Argon, 2003b), much higher than the prediction of the McClintock model.

Inside a single grain, a cleavage crack can keep propagating until the crack-tip stress intensity decreases to the critical level of crack stoppage (Qiao and Argon, 2003c). When the crack front encounters a grain boundary, usually the cracking process would be interrupted (Saeedvafa, 1992). Because the fracture surface must be misoriented across a boundary, additional crack growth driving force is needed to overcome the boundary toughness (Gell and Smith, 1967). For example, low-temperature cracking often stops at grain boundaries (Zikry and Kao, 1994) and it is generally accepted that grain-sized microcracks pre-exist in engineering materials (Anderson, 2004). At a high-angle grain boundary, under a quasi-static loading, the crack front behavior is quite uniform (Argon and Qiao, 2002). The crack front penetrates across the boundary simultaneously at a number of break-through points, forming a series of cleavage terrains in the grain ahead of the boundary (Qiao and Argon, 2003a). The borders of adjacent terrains are known as river markings. Due to the competition between the grain boundary separation and the river marking formation, the distance between the break-through points, w_{bt}, is insensitive to the crystallographic orientation (Chen and Qiao, 2008a). Such a regular break-through mode has been observed in various materials at grain boundaries (Chen et al., 2008; Chen and Qiao, 2007a,b, 2008b; Kong and Qiao, 2005; Qiao, 2003), twin boundaries (Chen et al., 2008), triple grain boundary junctions (Chen and Qiao, 2008c; Chen et al., 2009), as long as the sample thickness is sufficiently large (Qiao and Chen, 2008; Qiao and Kong, 2007; Qiao et al., 2008). Due to the fracture work required to separate the grain boundary, the local fracture toughness is increased to (Chen and Qiao, 2008a): $K_{gb0} = K_{cp}\sqrt{(\sin\theta + \cos\theta)/\cos^2\varphi + C \cdot \sin\theta \cdot \cos\theta/\cos\varphi}$, where K_{cp} is the fracture toughness of crystallographic plane; θ and ϕ are the twist and tilt misorientation angles, respectively; and C is a material constant, which is defined as $C = \beta k w_{bt}/(4G_{cp})$, with β being the ratio of the crack tip opening displacement to the cleavage front penetration depth, $G_{cp} = (1-\nu^2)K_{cp}^2/E$ the fracture resistance of crystallographic plane, and ν and E the Poisson's ratio and the modulus of elasticity, respectively. While K_{gb0} is typically 1–2 times larger than K_{cp}, it is smaller than K_{gb1}, and, therefore, cannot explain why in the near BDT temperature range the resistance of cleavage-like fracture is so high.

The regular break-through mode of grain boundary is observed in purely brittle materials at low temperature. In the transition zone, the grain boundary behavior can be highly nonuniform, which may induce additional fracture resistance. Similar nonuniform crack advance has been noticed in composite materials (Gao and Rice, 1989; Mower and Argon, 1995). When a cleavage crack grows in a brittle matrix, it cannot directly bypass the tough, strongly bonded reinforcements. The crack front must penetrate in between the reinforcements, with the rest of front sections being arrested locally. At the protruding front sections, the local crack growth driving force is smaller than that at the concave parts, and, thus, the overall energy intensity must increase with the crack front penetration depth. Such a toughing mechanism may also be achieved by a high-angle grain boundary, as will be discussed below.

2. Nonuniform crack advance across a high-angle grain boundary

Fig. 1 shows the fracture surface of a decarburized 1010 steel at −85 °C. The details of the experiment have been discussed elsewhere (Qiao and Argon, 2003b). At this temperature, it can be seen that the fracture inside each grain is in cleavage mode. A cleavage facet contains a number of river markings. However, the testing data showed that the fracture resistance was about 70 kN/m, much higher than the predictions of the McClintock model (1.5 kN/m). At room temperature, the fracture resistance of the same material was about 60 kN/m, and the fracture mode was purely fibrous. The fracture appearance transition occurred in the range of −55 to −40 °C. The fracture resistance transition temperature was below −150 °C. The difference between the fracture appearance transition temperature and the fracture toughness transition temperature was more than 100 °C.

An interesting phenomenon is that the river markings in most of the grains were radial. The river markings were typically formed in a small zone and then expanded to the entire grain. Clearly, the cleavage front behavior at grain boundary was nonuniform; otherwise the river markings should be parallel to each other.

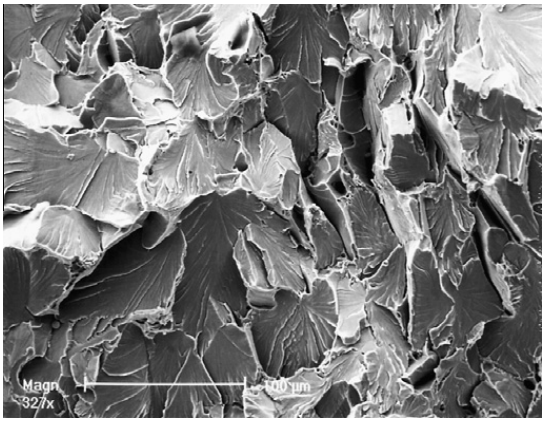

Fig. 1. SEM fractograpy of a decarburized 1010 steel at −85 °C. The crack propagates from the top to the bottom.

As depicted in Fig. 2(a), the cleavage crack first penetrates through a high-angle grain boundary in its central part, which will be referred to as break-through window (BTW) in the following discussion. Due to the crystallographic misorientation of the two grains across the grain boundary, the fracture surface must be twisted by θ as it bypasses the boundary. Inside a BTW, as shown in Fig. 1 and depicted in Fig. 2, the transmission of the fracture surface is quite smooth. The cleavage front advances from the grain behind the boundary (grain "A") to the grain ahead of the boundary (grain "B"), with the boundary piece being separated apart simultaneously. The separation of the grain boundary inside the BTW may be described as the quasi-mode-II fracture process in the McClintock model, and, thus, the local fracture toughness can be estimated as K_{gb1}.

Outside the BTW, the grain boundary does not yield immediately after the cleavage front penetration starts. When the crack front bows into grain "B" in the central part, the side sections of the grain boundary bridge the local fracture flanks together, somewhat similar to a pair of tough reinforcements in a composite material. Along the curved crack front, the local crack growth driving force is a function of the location, x_1. The lowest crack growth driving force is at the center of the BTW. The highest crack growth driving force occurs outside the BTW at the persistence grain boundary, where the crack growth is locally stopped. Since the crack front must overcome the local fracture toughness, K_{gb1}, in the BTW to penetrate into grain "B", the overall stress intensity along the entire grain boundary, which can be regarded as the average of the minimum and the maximum local crack growth driving forces, must be higher than K_{gb1}. As the effective crack front penetration depth increases, the BTW expands along the boundary and the required crack growth driving force becomes larger; that is:

$$G = R, \tag{1}$$

must be satisfied to further increase the effective crack length, where G is the overall crack growth driving force, and R is the fracture resistance offered by the grain boundary.

Along a curved crack font, the local stress intensity can be calculated as (Bower and Ortiz, 1991):

$$K(x_1) = K_{ref} + \int_\Omega H\left(s, \vec{\xi}\right) F(\xi_1) d\Omega, \tag{2}$$

where (x_1, x_2) and (ξ_1, ξ_2) are global and local coordinate systems, respectively, with subscript "1" indicating the direction parallel to the grain boundary and "2" indicating the crack growth direction; $K_{ref} \approx K_{gb1}$ is the stress intensity factor for a homogeneous reference system where grain "B" has the same crystallographic orientation as grain "A"; Ω indicates the intersection line of the grain boundary and the fracture surface; F is the bridging force required to pin down the local fracture flanks and is nonzero only outside the BTW; and $H(s, \vec{\xi}) = \sqrt{2/\pi^3}\sqrt{-\xi_2}/(s^2 + \xi_2^2)$ is a weight function, with $s = |x_1 - \xi_1|$ (Ulfyand, 1965). The average stress intensity along the crack font can be obtained as:

$$\bar{K} = K_{ref} + \frac{1}{D_g}\int_{-D_g/2}^{D_g/2}\int_\Omega H\left(s, \vec{\xi}\right) F(\xi_1) \mathrm{d}\Omega \mathrm{d}x_1. \tag{3}$$

The shape of the penetrating crack front inside the BTW can be assumed as a part of a circle, since the radial pattern of river markings is quite regular (Fig. 1). Denote the radius of the circle as r_0 and the width of BTW as W_{bt}. The penetration depth of the crack front, which can be taken as the effective crack growth length, is $\Delta a = r_0 - \sqrt{r_0^2 - W_{bt}^2/4}$. If the grain boundary did not exist, the fracture flanks should be entirely separate. The local crack opening distance Δa away from the crack front is $V = 2\bar{K}(1-\nu)\sqrt{\Delta a/(2\pi\mu^2)}$ (Ulfyand, 1965), where ν is the Poisson's ration and μ is the shear modulus. In order to pin down the fracture flanks, the bridging force in the persistence grain boundary, $F(x_1)$, must causes a deflection of $-V$; that is:

$$\int_\Omega U(\vec{x}, \vec{\xi}) F(\xi_1) \mathrm{d}\Omega = -\frac{\mu V}{1-\nu}, \tag{4}$$

where $U(\vec{x}, \vec{\xi}) = -(1/\pi^2\rho)\arctan\left[2\sqrt{x_2\xi_2/\rho^2}\right]$ and $\rho = |\vec{x} - \vec{\xi}|$.

Note that the value of r_0 is not arbitrary. On the one hand, with a given Δa, as r_0 decreases, the width of persistent grain boundary increases and the change in crack-front contour is "steeper", both of which tend to increase the local fracture resistance. To minimize the fracture resistance, the radius of penetrating crack front should be as large as possible. On the other hand, if the

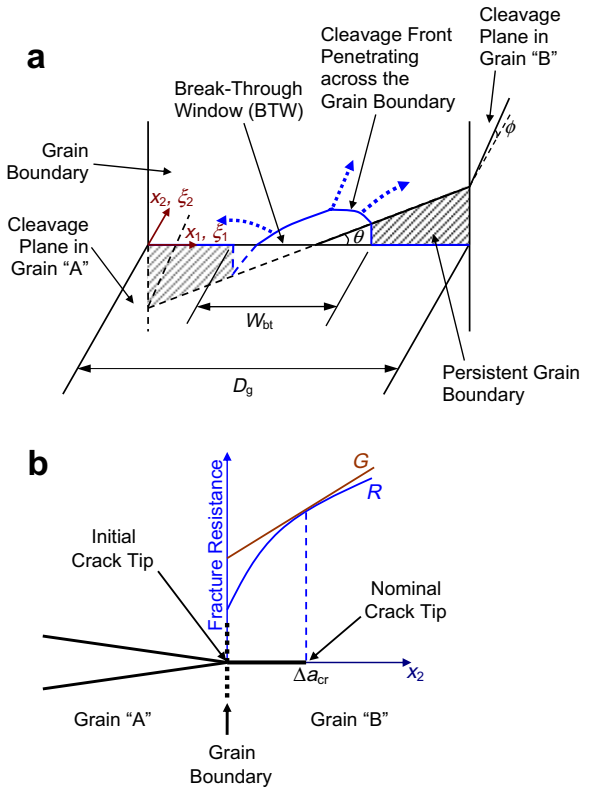

Fig. 2. Schematics of nonuniform cracking across a high-angle grain boundary: (a) the three-dimensional view, and (b) the side view.

width of persistent grain boundary is too small, the required bridging force would exceed the shear strength of the grain boundary, k, and, consequently, the cleavage front is no longer stable. At the equilibrium condition, the optimum value of the radius of penetrating crack front, r_f, can be calculated through:

$$\max\{F(x_1)\} = k \cdot h_1, \tag{5}$$

where h_1 is the height of the persistent grain boundary.

Based on Eqs. (1)–(5), if the critical BTW width, W_{cr}, is known, the peak resistance offered by the grain boundary to crack advance can be calculated as:

$$G_{gb} = R_{gb}, \tag{6}$$

where $R_{gb} = (1-\nu^2)\bar{K}_{cr}^2/E$, with E being the modulus of elasticity and $\bar{K}_{cr}$ is the average stress intensity along the boundary when $W_{bt} = W_{cr}$.

3. Unstable crack advance across a high-angle grain boundary

As discussed above, the persistent grain boundary behaviors are somewhat similar to that of tough reinforcements in a composite material. It increases the fracture toughness through the crack trapping effect, as shown in Eq. (2). In a composite material, the required crack growth driving force to overcome the crack trapping effect increases monotonically with the content of the reinforcements, W_r/D_r (Xu et al., 1998; Rice, 1985), where W_r and D_r are the average size and the center-to-center distance of the reinforcements, respectively.

At a grain boundary, if the BTW width is too small, the front behavior is governed by the persistence grain boundary, and the global crack growth can be prohibitively difficult. At the beginning stage of crack growth, the cleavage front can advance only in the BTW. As the fracture loading becomes larger, the front penetration depth increases, and the BTW expands along the boundary. The increase rate of the crack growth driving force can be calculated as:

$$\frac{\partial G}{\partial W_{bt}} = \frac{2(1-\nu^2)\bar{K}_{cr}}{E}\frac{\partial \bar{K}_{cr}}{\partial W_{bt}}. \tag{7}$$

The total fracture work for the BTW to expand by W_{bt} is:

$$W = W_{gb} + G_B \cdot A_B, \tag{8}$$

where W_{gb} is the work required to separate apart the grain boundary in BTW; $G_B = G_{cry}/(\cos\theta \cdot \cos\phi)$ is the effective surface free energy of grain "B", with G_{cry} being the effective surface free energy of crystallographic plane; and A_B is the area of the fracture surface in grain "B" within the BTW. The value of W_{gb} can be calculated as:

$$W_{gb} = \int_0^{W_{bt}/2} k\varepsilon_0 (x_1 \tan\theta)^2 dx_1 = \frac{k\varepsilon_0 \tan^2\theta}{24} W_{bt}^3, \tag{9}$$

with $\varepsilon_0 = k/\mu$ being the critical shear strain of grain boundary failure. Substitution of Eq. (9) into (8) gives:

$$W = \frac{k\varepsilon_0 \tan^2\theta}{24} W_{bt}^3 + G_B \cdot A_B. \tag{10}$$

According to the basic concept of fracture mechanics, the resistance of grain boundary to BTW expansion can then be obtained as:

$$R_{bt} = \frac{\partial W}{\partial W_{bt}} = \frac{k\varepsilon_0 \tan^2\theta}{8} W_{bt}^2 + G_B \frac{\partial A_B}{\partial W_{bt}}. \tag{11}$$

Because the value of k is much larger than G_B, the first term at the right-hand side of Eq. (11) dominates R_{bt}. It can be seen that R_{bt} increases with W_{bt}. As depicted in Fig. 2, when the crack front keeps penetrating into grain "B", the effective crack growth distance, Δa, rises, associated with the expansion of BTW. Due to the increase in fracture resistance, the fracture loading must be increased to drive the cleavage front further across the grain boundary. Initially, because the BTW width is small, the persistent grain boundary cannot be abruptly broken through; i.e. the crack front advance in the BTW is stable. When the BTW expands by a small incremental amount, while the crack growth driving force is higher, the fracture resistance increases with a higher rate, and, consequently, the crack front would stop in grain "B" until the overall stress intensity is further increased. Such a process is similar to the well known R-curve behavior.

The increase rate of the resistance to BTW expansion is:

$$\frac{\partial R_{bt}}{\partial W_{bt}} = \frac{k\varepsilon_0 \tan^2\theta}{4} W_{bt} + G_B \frac{\partial^2 A_B}{\partial^2 W_{bt}}, \tag{12}$$

With the increase of the BTW width, eventually the increase rate of crack growth driving force would be higher than the increase rate of the fracture resistance. Under this condition, as the BTW expands slightly, even without any input energy, the crack growth driving force would exceed the fracture resistance, and as the crack advances the difference between them increases. Thus, the crack front becomes unstable and the persistent grain boundary would be separated apart in a catastrophic manner. At the critical point, i.e. when $\Delta a = \Delta a_{cr}$ and $W_{bt} = W_{bt0}$:

$$\frac{\partial G}{\partial W_{bt}} = \frac{\partial R_{bt}}{\partial W_{bt}}, \tag{13}$$

where Δa_{cr} and W_{bt0} are the critical crack growth distance and the critical BTW width, respectively. Substitution of Eqs. (7) and (12) into (13) gives:

$$\frac{2(1-\nu^2)\bar{K}_{cr}}{E}\frac{\partial \bar{K}_{cr}}{\partial W_{bt}} = \frac{k\varepsilon_0 \tan^2\theta}{4} W_{bt} + G_B \frac{\partial^2 A_B}{\partial^2 W_{bt}}. \tag{14}$$

Combination of Eqs. (2)–(5), and (14) provides the solutions for the critical BTW width, W_{bt0}, and the critical energy release rate of grain boundary, G_{gb}.

4. Results and discussion

Eqs. (2)–(5), and (14) were solved numerically. Experimental data of the material parameters of the decarbonized 1010 steel shown in Fig. 1 were used (Qiao and Argon, 2003b). The average grain size, D_g, was set to 75 μm. The modulus of elasticity (E) and the yield strength (Y) were taken as 211 GPa and 200 MPa, respectively. The shear modulus was set to $E/\sqrt{3}$, and the shear strength was set to $Y/\sqrt{3}$. The Poisson's ratio was 0.3. The critical

energy release rate of crystallographic plane was taken as 800 N/m (Qiao and Argon, 2003c). The effective fracture resistance in BTW was assumed to be 1.5 kN/m (McClintock, 1997).

In order to avoid the convergence problem, the Ritz method was used to convert Eq. (4), which is a type-I Fredholm integral equation, to a set of algebra equations, by assuming that $F(x_1) = \sum_{i=0}^{3} \alpha_i x_1^i$, where α_i are unknown coefficients. For the domain of Ω, the grain boundary containing the BTW and its four nearest neighbors were taken into consideration. Including higher orders terms in the expression of bridging force or considering more grains would cause only negligible variations in the numerical results of W_{bt0} and G_{gb}.

Figs. 3 and 4 show the results of the grain boundary toughness, $K_{gb} = \sqrt{EG_{gb}/(1-\nu^2)}$, and the critical width of break-through window. The numerical data indicate that K_{gb} is quite insensitive to the values of E and μ, as long as ε_0 is constant. As E is varied in the range of 70 MPa to 1 GPa, K_{gb} changes by only less than 5%, suggesting that the grain boundary toughness is not dependent on the

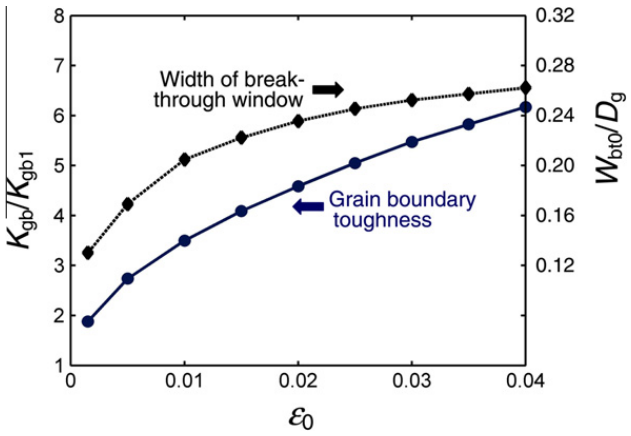

Fig. 3. The grain boundary toughness (K_{gb}) and the critical width of break-through window (W_{bt0}) as functions of the grain boundary ductility (ε_0). Both of the twist and tilt crystallographic misorientation angles are set to 22.5°.

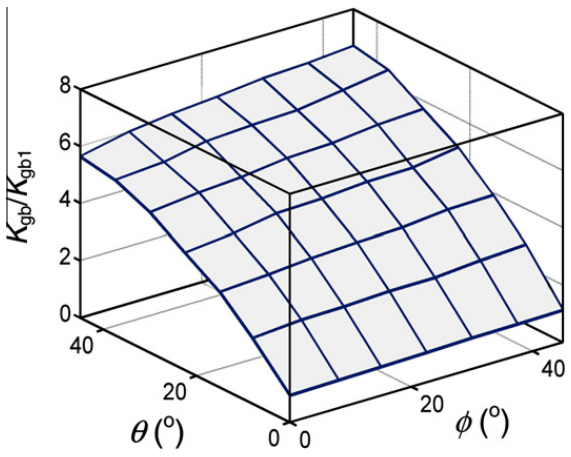

Fig. 4. The grain boundary toughness as a function of the crystallographic misorientation. The value of ε_0 is set to 0.02.

elastic properties of the material. The influence of ν is also secondary. When ν is changed in the range from 0.25 to 0.35, the variation in K_{gb} is less than 6%, as it should be, since, as discussed above, K_{gb} is insensitive to the elastic properties of the material and in the framework of linear elastic fracture mechanics (LEFM) the critical energy release rate and the critical stress intensity factor are equivalent to each other. Note that, because the model is scalable, the dominant geometrical factor is W_{bt}/D_g, instead of the absolute values of W_{bt} and D_g.

When the grain boundary ductility, ε_0, is varied, according to Fig. 3, the grain boundary toughness changes considerably, so does the critical BTW width. When ε_0 is small, the material is relatively brittle, and the total work required to separate apart the persistent grain boundary is negligible. Thus, the side sections of grain boundary do not offer much additional resistance to the BTW expansion and the crack growth, and the overall fracture toughness, K_{gb}, is governed by the crack front behavior inside BTW, close to K_{gb1}. In fact, if the resistance of the persistent grain boundary to the BTW expansion is zero the entire grain boundary would be broken through uniformly by the cleavage front, which converges to the McClintock model.

With the increasing of ε_0, the crack trapping effect of the persistent grain boundary becomes increasingly pronounced, and the overall fracture toughness is significantly higher than the local fracture toughness in BTW. The numerical calculation predicts a nearly 800% increase in K_{gb} when ε_0 is changed from 0% to 4%. The value of K_{gb} is most sensitive to ε_0 when ε_0 is relatively small. As ε_0 increases from 0% to 1%, the overall fracture toughness increases by nearly 350%. When ε_0 is relatively large, its influence on fracture is reduced.

The variation in fracture toughness is accompanied by the change in critical BTW width, which increases with ε_0 monotonically. Similar to the fracture toughness, W_{bt0} increases with ε_0 with a decreasing rate; that is, it is more sensitive to the grain boundary ductility when ε_0 is smaller. In the range of ε_0 under investigation, W_{bt0} is around 10–25% of the grain size, D_g. Note that since the model is scalable, the calculation result of the critical BTW width increases linearly with the grain size. Therefore, varying the absolute value of D_g would not cause any change in the results of K_{gb}.

From the experimental observation, the final BTW width is nearly 20–25% of the grain size. According to Fig. 3, this corresponds to a K_{gb} value 5–6 times higher than K_{gb1}. Based on the McClintock model, K_{gb1} can be taken as 18 MPa $m^{1/2}$ (McClintock, 1997), and, thus, by taking into account the crack trapping effect associated with the non-uniform front behavior at grain boundary, the overall fracture toughness increases to 90–110 MPa $m^{1/2}$, close to but slightly lower than the experimental data. The model is conservative because it analyzes the most energetically favorable break-through process of crack front, with the front radius being optimized. In reality, the actual r_0 would be different from the optimum value, due to the dynamic effect, the constraints of adjacent grains, as well as the undercutting and bending of fracture ligaments. Furthermore, in a polycrystalline sample, along the crack front

there would be grains of misorientation angles larger than 22.5°, which offers higher resistance to crack advance. From Fig. 4, it can be seen that K_{gb} increases with both θ and ϕ. However, the influence of the tilt angle, ϕ, is only secondary, since the factor of ϕ comes in by affecting G_B. When θ is 0, there is no twist mismatch between grains "A" and "B", and the persistent grain boundary does not exist. Thus, the result is reduced to the case of uniform front advance process analyzed by the McClintock model. As the twist misorientation becomes nontrivial, the crack trapping effect leads to a much higher fracture toughness. The value of $dK_{gb}/d\theta$ is higher when θ is smaller. These results are consistent with the previous experimental data of fracture resistance of high-angle grain boundaries (Qiao and Argon, 2003b).

Since the dominant factor that affects the overall fracture toughness are ε_0 and θ, K_{gb} may be calculated by a closed form expression:

$$K_{gb} = f_1(\varepsilon_0) \cdot f_2(\theta), \tag{15}$$

where $f_1(\varepsilon_0) = \sum_i \eta_i \hat{\varepsilon}_0^i$ and $f_2(\theta) = \sum_i \varsigma_i \theta^i$ are two polynomials, with $\hat{\varepsilon}_0 = \varepsilon_0 \times 100\%$ and $i = 0, 1, 2$. Through a regression analysis of the numerical results, the coefficients are obtained as $\eta_i = \{1, 2.434, -0.286\}$ and $\zeta_i = \{1, 2.042, -0.0019\}$. For a field of randomly misoriented grains, θ distributes uniformly in the range from 0 to 45°, and f_2 may be reduced to a constant of 4.6.

5. Concluding remarks

In summary, the nonuniform cleavage cracking process after extended plastic deformation at grain boundary, which occurs when the fracture appearance transition temperature is higher than the fracture resistance transition temperature, is analyzed. Due to the difficulty in plastic shearing along the grain boundary, when the crack growth driving force is relatively low, the crack front can penetrate through the grain boundary only in the central part, leading to the formation of a break-through window and the radial river markings. The critical condition of the transition from stable break-through window expansion to unstable crack advance is determined not only by the magnitude of crack growth driving force, but also by its increasing rate. The persistent grain boundary outside the break-through window causes a significant crack trapping effect, which can result in a large increase in grain boundary toughness by 5–6 times, compared with the local fracture toughness inside the break-through window. The overall fracture resistance offered by a high-angle grain boundary is quite insensitive to the elastic properties and the grain size. The dominant factors are the grain boundary ductility as well as the crystallographic misorientation, particularly the twist misorientation.

Acknowledgement

This work was supported by the Department of Energy under Grant No. DE-FG02-07ER46355.

References

Anderson, T.L., 2004. Fracture Mechanics. CRC Press.
Argon, A.S., Qiao, Y., 2002. Resistance of cleavage cracking of high-angle bicrystal grain boundaries in Fe–Si alloy. Philos. Mag. A 82, 3333–3348.
Bower, A.F., Ortiz, M., 1991. A three dimensional analysis of crack trapping and bridging by tough particles. J. Mech. Phys. Solids 39, 815–858.
Chen, J., Qiao, Y., 2007a. Secondary cracking at grain boundaries in silicon thin films. Scripta Mater. 57, 1069–1072.
Chen, J., Qiao, Y., 2007b. Mixed-mode cleavage front branching at a high-angle grain boundary. Scripta Mater. 56, 1027–1030.
Chen, J., Qiao, Y., 2008a. Characteristic length scale in cleavage cracking across high-angle grain boundary. Comput. Mater. Sci. 42, 664–669.
Chen, J., Qiao, Y., 2008b. Interaction of cleavage ridges with grain boundaries in polysilicon films. Appl. Phys. A 91, 127–130.
Chen, J., Qiao, Y., 2008c. Cleavage cracking across triple grain boundary junctions in free-standing silicon thin films. J. Mater. Res. 23, 1647–1651.
Chen, J.H., Wang, G.Z., Yan, C., Ma, H., Zhu, L., 1997. Advances in the mechanism of cleavage fracture of low alloy steel at low temperature. Part I: critical event. Int. J. Fracture 83, 105–120.
Chen, J., Lu, W., Qiao, Y., 2008. Cleavage cracking across twin boundaries in free-standing silicon thin films. Appl. Phys. A 91, 663–666.
Chen, J., Lu, W., Qiao, Y., 2009. Resistance of grain boundary array to cleavage cracking in free-standing thin film. Mech. Mater. 41, 131–138.
Colangelo, V.J., Heiser, F.A., 1987. Analysis of Metallurgical Failures. Wiley Interscience.
Dodd, B., Bai, Y., 1987. Ductile Fracture and Ductility: With Applications to Metalworking. Academic Press.
Gao, H., Rice, J.R., 1989. A first order perturbation analysis of crack trapping by arrays of obstacles. J. Appl. Mech. 56, 828–836.
Gell, M., Smith, E., 1967. The propagation of cracks through grain boundaries in polycrystalline 3% silicon–iron. Acta Meter. 15, 253–258.
Hull, D., 1999. Fractography. Cambridge University Press.
Kang, Y., 1999. Experimental analysis for some interfacial mechanics problems. Mech. Pract. 21, 990302.
Kong, X., Qiao, Y., 2005. Crack trapping effect of persistent grain boundary islands. Fatigue Fract. Eng. Mater. Struct. 28, 753–758.
Lyman, T., 1969. Forming. Metals Handbook, vol. 4. American Society of Metals, Metals Park, OH, p. 33.
McClintock, F.A., 1997. A three dimensional model for polycrystalline cleavage and problems in cleavage after extended plastic flow or cracking. In: Chan, K.S., Irwin, George R. (Eds.), Symposium on Cleavage Fracture. The Minerals, Metals, and Materials Society, Warrendale, PA, pp. 81–94.
McClintock, F.A., Argon, A.S., 1966. Mechanical Behavior of Materials. Addison-Wesley.
Mower, T.M., Argon, A.S., 1995. Experimental investigations of crack trapping in brittle heterogenous solids. Mech. Mater. 19, 343–364.
Neimitz, A., Galkiewicz, J., 2010. The analysis of fracture mechanisms of ferritic steel 13HMF at low temperatures. J. ASTM Int. 7, JAI102470.
Neimitz, A., Galkiewicz, J., Dzioba, I., 2010. The ductile to cleavage transition in ferritic Cr–Mo–V steel: a detailed microscopic and numerical analysis. Eng. Fract. Mech. 77, 2504–2526.
Nemat-Nasser, S., 1981. Three-Dimensional Constitutive Relations and Ductile Fracture. Elsevier.
Qiao, Y., 2003. Modeling of resistance curve of high-angle grain boundary in Fe–3wt%Si alloy. Mater. Sci. Eng., A 361, 350–357.
Qiao, Y., Argon, A.S., 2003a. Cleavage cracking resistance of high angle grain boundaries in Fe–3wt%Si alloy. Mech. Mater. 35, 313–331.
Qiao, Y., Argon, A.S., 2003b. Cleavage crack-growth-resistance of grain boundaries in polycrystalline Fe–2wt%Si alloy: experiments and modeling. Mech. Mater. 35, 129–154.
Qiao, Y., Argon, A.S., 2003c. Brittle-to-ductile fracture transition in Fe–3wt%Si single crystals by thermal crack arrest. Mech. Mater. 35, 903–912.
Qiao, Y., Chen, J., 2008. Resistance of through-thickness grain boundaries to cleavage cracking in silicon thin films. Scripta Mater. 59, 251–254.
Qiao, Y., Kong, X., 2007. On size effect of cleavage cracking in polycrystalline thin films. Mech. Mater. 39, 746–752.
Qiao, Y., Chen, J., Kong, X., Chakravarthula, S.S., 2008. Energy equilibrium of cleavage front transmission across a high-angle grain boundary in a free-standing silicon thin film. Eng. Fract. Mech. 75, 2444–2452.

Rice, J.R., 1985. First order variation in elastic fields due to variation in location of a planar crack front. J. Appl. Mech. 52, 571–579.
Saeedvafa, M., 1992. Orientation dependence of fracture in copper bicrystals with symmetric tilt boundaries. Mech. Mater. 13, 295–311.
Ulfyand, Y.S., 1965. Survey of Articles on the Application of Integral Transforms in Theory of Elasticity. University of North Carolina, Raleigh, NC.
Wiesner, C.S., 1996. The Local Approach to Cleavage Fracture. Woodhead Publishing.
Wu, X.Y., Ramesh, K.T., Wright, T.W., 2003. The dynamic growth of a single void in a viscoplastic material under transient hydrostatic loading. J. Mech. Phys. Solids 51, 1–26.
Xu, G., Bower, A.F., Ortiz, M., 1998. The influence of crack trapping on the toughness of fiber reinforced composites. J. Mech. Phys. Solids 46, 1815–1833.
Zikry, M.A., Kao, M., 1994. High angle grain boundary effects and microstructural failure mechanisms in crystalline materials. Comput. Mater. Model. 42, 71–101.